IOPscience iopscience.iop.org

Home Search Collections Journals About Contact us My IOPscience

Collective dynamics in crystalline polymorphs of $ZnCl_2$: potential modelling and inelastic neutron scattering study

This article has been downloaded from IOPscience. Please scroll down to see the full text article.

2005 J. Phys.: Condens. Matter 17 6179

(http://iopscience.iop.org/0953-8984/17/39/006)

View the table of contents for this issue, or go to the journal homepage for more

Download details:
IP Address: 129.252.86.83
The article was downloaded on 28/05/2010 at 05:59

Please note that terms and conditions apply.

INSTITUTE OF PHYSICS PUBLISHING JOURNAL OF PHYSICS: CONDENSED MATTER

J. Phys.: Condens. Matter **17** (2005) 6179–6192 doi:10.1088/0953-8984/17/39/006

Collective dynamics in crystalline polymorphs of $ZnCl_2$: potential modelling and inelastic neutron scattering study

A Sen[1], **Mala N Rao, R Mittal and S L Chaplot**[2]

Solid State Physics Division, Bhabha Atomic Research Centre, Trombay, Mumbai 400085, India

E-mail: chaplot@magnum.barc.ernet.in

Received 4 July 2005, in final form 24 August 2005
Published 16 September 2005
Online at stacks.iop.org/JPhysCM/17/6179

Abstract

We report a phonon density of states measurement of α-$ZnCl_2$ using the coherent inelastic neutron scattering technique and a lattice dynamical calculation in four crystalline phases of $ZnCl_2$ using a transferable interatomic potential. The model calculations agree reasonably well with the available experimental data on the structures, specific heat, Raman frequencies and their pressure variation in various crystalline phases. The calculated results have been able to provide a fair description of the vibrational as well as the thermodynamic properties of $ZnCl_2$ in all its four phases.

1. Introduction

Among the metal halides of form MX_2 (M: metal, X: halide), $ZnCl_2$ continues to draw attention in current research for several reasons. Firstly, the crystalline $ZnCl_2$ has four structurally determined polymorphs [1, 2] at the ambient pressure, namely α-$ZnCl_2$ ($I\bar{4}2d$, $Z = 4$), β-$ZnCl_2$ ($P2_1/n$, $Z = 12$), γ-$ZnCl_2$ ($P4_2/nmc$, $Z = 2$) and δ-$ZnCl_2$ ($Pna2_1$, $Z = 4$) in which the Zn atom is tetrahedrally coordinated with Cl atoms. Secondly, $ZnCl_2$ displays unique phase transitions upon compression as well as pressure release. For instance, the four-coordinated α-$ZnCl_2$ transforms into a six-coordinated $CdCl_2$-like phase at 2.1 GPa, which further converts into four-coordinated γ-$ZnCl_2$ upon decompression [3]. Thirdly, molten $ZnCl_2$, which is commercially used as a solvent and catalyst in the hydro cracking of coal slurries and heavy crude oil fractions [4], typifies high viscosity [5–7], low ionic diffusivities [8], and very low electric conductivity [9] due mainly to its non-uniform polymeric network linkage [10]. Further, liquid $ZnCl_2$ has the ability to supercool into a glass [11] at a relatively low glass transition temperature ($T_g = 375$ K). Finally, $ZnCl_2$ glass, which is intermediate between

[1] Present address: Department of Physics, Indian Institute of Technology, Kanpur 208016, India.
[2] Author to whom any correspondence should be addressed.

Table 1. Group theoretical classification of zone-centre phonon modes in various crystalline polymorphs of $ZnCl_2$. Raman and infra-red active phonon branches are indicated within the bracket by R and ir respectively.

Phase	Crystal system	Space group	Z	Group theoretical classification at zone-centre
α	Tetragonal	$I\bar{4}2d$	4	$A_1(R) + 2A_2 + 2B_1(R) + 3B_2(R, ir) + 5E(R, ir)$
β	Monoclinic	$P2_1/n$	12	$27A_g(R) + 27A_u(ir) + 27B_g(R) + 27B_u(ir)$
γ	Tetragonal	$P4_2/nmc$	2	$A_{1g}(R) + 2A_{2u}(ir) + 2B_{1g}(R) + B_{2u}(ir) + 3E_g(R) + 3E_u(ir)$
δ	Orthorhombic	$Pna2_1$	4	$9A_1(R, ir) + 9A_2(R) + 9B_1(R, ir) + 9B_2(R, ir)$

strong (e.g. SiO_2) and fragile (e.g. CKN) glasses, finds its potential use as a low-loss optical transmission medium in the near-infrared region [12].

All the crystalline phases of $ZnCl_2$ at ambient pressure are formed by the network of $ZnCl_4$ tetrahedra sharing their corners. But this network is rather soft (unlike SiO_2 or BeF_2), resulting in a strongly hybridized character for the normal modes of vibration [11]. Further, in the low frequency range ($<20\,cm^{-1}$), where the collective acoustic modes are expected to dominate the vibrational density of states, liquid $ZnCl_2$ exhibits a prominent boson peak [13, 14] reflecting its more complex microstructure. Ribero *et al* [15] examined the nature of instantaneous normal modes in the atomic motion of liquid $ZnCl_2$, which involve the coupled vibration of several quasi-molecular $ZnCl_4$ units of the network and has the local torsional character.

Although molecular dynamics (MD) and Monte Carlo (MC) simulations have been reported for glassy as well as molten $ZnCl_2$, the need for a realistic interatomic potential has remained unfulfilled [16]. The present work is primarily intended to make an attempt in formulating an effective transferable interatomic potential that can be applied to any of the polymorphs of $ZnCl_2$ with equal ease. Angell *et al* [17] have already suggested that there is little distinction between the glassy and the crystalline behaviour of $ZnCl_2$ so far as the dynamics is concerned. They further opined that the short time dynamics of liquid $ZnCl_2$ near its melting point ($T_m = 593$ K) might be regarded as solid-like in character. Later on, x-ray diffraction measurements of molten $ZnCl_2$ by Triolo and Narten [18] favoured this argument strongly. Anomalously low enthalpy and volume changes on fusion are supposed to be behind the resemblance of $ZnCl_2$ melt to the crystalline structure [4]. An extensive neutron diffraction study by Desa *et al* [19] further showed that vitreous $ZnCl_2$ has a distorted close packed array of Cl atoms in which Zn atoms are randomly distributed in the tetrahedral sites. Numerous such studies undoubtedly imply that if we are able to understand the dynamical properties of crystalline polymorphs of $ZnCl_2$, microscopic interpretation for glassy and molten phases will also be robust. In the present work we have also determined the phonon density of states in the α-phase by coherent inelastic neutron scattering. The potential model calculation is found to be in fair agreement with the neutron data.

2. Crystal structure

Till 1961, it was commonly believed that the ambient stable phase of $ZnCl_2$ had a layered structure in which each Zn atom was coordinated to six Cl atoms to form regular octahedra with van der Waals bonding between the layers [20]. Later investigations proved that $ZnCl_2$ has bonding based on a tetrahedral framework. Initially three solid phases of $ZnCl_2$ were known crystallographically. These were α, β and γ polymorphs of $ZnCl_2$ belonging to monoclinic and tetragonal crystal classes (table 1). While α and β phases have cristobalite type three dimensional networks of corner linked tetrahedra [1], γ-$ZnCl_2$ crystallizes to a layered structure of cross linking tetrahedra as in the case of red HgI_2 [21]. However, in 1978, Brynestad and

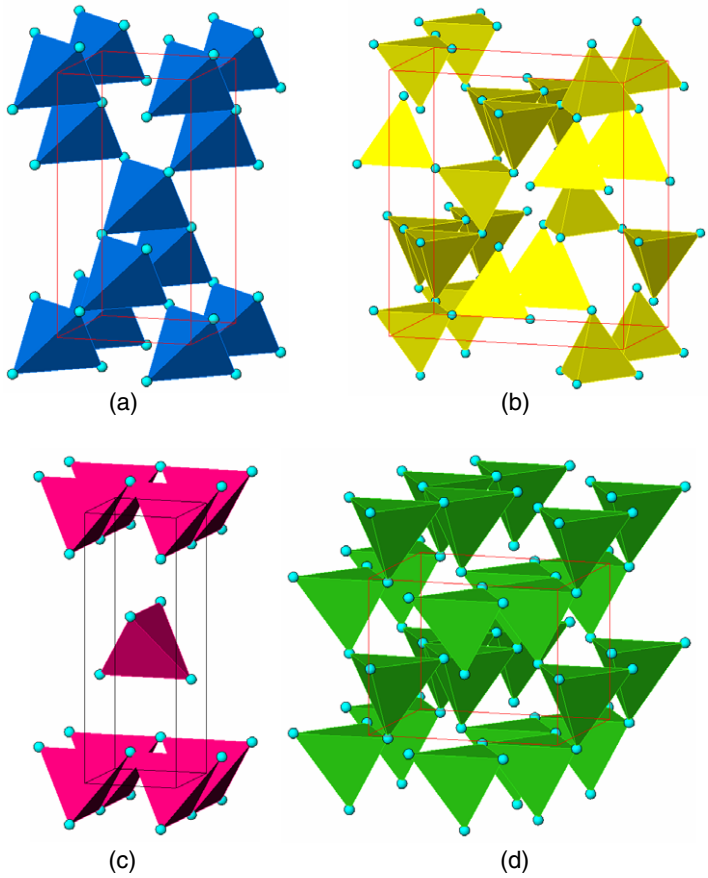

Figure 1. Crystal structures of polymorphs of $ZnCl_2$, namely (a) α-$ZnCl_2$, (b) β-$ZnCl_2$, (c) γ-$ZnCl_2$ and (d) δ-$ZnCl_2$. The small circles represent Cl atoms, while Zn atoms are located inside (not visible here) the $ZnCl_4$ tetrahedra.

(This figure is in colour only in the electronic version)

Yakel [2, 22] pointed out that all three modifications are rather the result of water contamination and that purely anhydrous $ZnCl_2$ has an orthorhombic unit cell containing corner linked $ZnCl_4$ tetrahedra. This orthorhombic phase has been referred to as δ-$ZnCl_2$ in various papers [3, 19]. Figure 1 suggests that the close packed layers in δ-$ZnCl_2$ are horizontal. Further, temperature has a significant impact [23] on the structure of $ZnCl_2$. While rapid cooling of the melt (or devitrification of the glass) produces the α-phase, slow cooling of the melt favours the formation of β-$ZnCl_2$. On the other hand, concentrated solution yields the γ-phase upon crystallization.

3. Experiments and data analysis

Experimental studies involving crystalline $ZnCl_2$ encounter difficulties because of its extreme hygroscopicity. The reagent grade chemical $ZnCl_2$ (purity 98%), purchased from Merck Chemical Co. (Germany) was dried for a period of 8 h. It was then exposed in the glove box under dry argon atmosphere for transferring into different containers. About 30 g of the polycrystalline $ZnCl_2$ sample so obtained was placed in a thin walled aluminium sample

Table 2. Transferable potential parameters for $ZnCl_2$ polymorphs.

R (Å)		C_{ij} (eV Å^6)					
Zn	Cl	Zn–Zn	Zn–Cl	Cl–Cl	D (eV)	n (Å^{-1})	r_0 (Å)
1.03	2.52	20	135	550	3.00	4.60	2.30

Table 3. Lattice constants and position parameters for α-$ZnCl_2$. For the space group $I\bar{4}2d$, Zn atoms are located at (0, 0, 0) and $\left(\frac{1}{2}, 0, \frac{3}{4}\right)$ while Cl atoms are located at general positions of $\left(x, \frac{1}{4}, \frac{1}{8}\right)$, $\left(\bar{x}, \frac{3}{4}, \frac{1}{8}\right)$, $\left(\frac{1}{4}, \bar{x}, \frac{7}{8}\right)$, $\left(\frac{3}{4}, x, \frac{7}{8}\right)$ respectively.

	This work	Experimental data [1]
a (Å)	5.406	5.410
c (Å)	10.415	10.300
V (Å^3)	304.34	301.46
x	0.24	0.25

Table 4. Lattice constants and position parameters for β-$ZnCl_2$. For the space group $P2_1/n$, Zn and Cl atoms are located at general positions of (x, y, z), $\left(\bar{x} + \frac{1}{2}, y + \frac{1}{2}, \bar{z} + \frac{1}{2}\right)$, $(\bar{x}, \bar{y}, \bar{z})$, $\left(x + \frac{1}{2}, \bar{y} + \frac{1}{2}, z + \frac{1}{2}\right)$ respectively.

	This work			Experimental data [1]		
a (Å)	6.519			6.500		
b (Å)	11.330			11.300		
c (Å)	12.272			12.300		
β (deg)	89.8			90.0		
V (Å^3)	906.43			903.43		
Atom	x	y	z	x	y	z
Zn	0.165	0.167	0.065	0.167	0.167	0.063
Zn	0.166	0.499	0.186	0.167	0.500	0.188
Zn	0.666	0.667	0.187	0.667	0.667	0.188
Cl	0.328	0.003	0.127	0.333	0.000	0.125
Cl	0.326	0.334	0.124	0.333	0.333	0.125
Cl	0.335	0.663	0.128	0.333	0.667	0.125
Cl	0.836	0.167	0.127	0.833	0.167	0.125
Cl	0.835	0.503	0.127	0.833	0.500	0.125
Cl	0.828	0.831	0.122	0.833	0.833	0.125

holder of circular shape for the inelastic neutron scattering (INS) studies. Another cylindrical vanadium can was made use of for taking the neutron diffraction pattern of the same sample. Neutron powder diffraction confirmed that the sample belongs to the α-phase. The structural refinements of the powder data were carried out using the Rietveld profile refinement method with the program DBWS 9411 [24]. The cell constants and atomic coordinates refined from the data recorded at 300 K are in close agreement with the reported data [1].

Inelastic neutron scattering measurements were carried out at 300 K using a medium resolution triple-axis spectrometer [25] at the Dhruva Reactor, Trombay. The instrument used a monochromated beam of neutrons produced by diffraction from the (111) planes of a copper crystal. Neutrons scattered inelastically by the sample were again diffracted by a pyrolytic graphite (002) analyser and subsequently detected in a $^{10}BF_3$ proportional counter. All the measurements were made in the energy loss mode with constant wavevector transfer (**Q**). The

Table 5. Lattice constants and position parameters for γ-$ZnCl_2$. For the space group $P4_2/nmc$, Zn atoms are located at (0, 0, 0) and $\left(\frac{1}{2}, \frac{1}{2}, \frac{1}{2}\right)$ while Cl atoms are located at general positions of $\left(0, \frac{1}{2}, z\right)$, $\left(0, \frac{1}{2}, z+\frac{1}{2}\right)$, $\left(\frac{1}{2}, 0, \bar{z}+\frac{1}{2}\right)$, $\left(\frac{1}{2}, 0, \bar{z}\right)$ respectively.

	This work	Experimental data [1]
a (Å)	3.733	3.700
c (Å)	10.859	10.670
V (Å^3)	151.31	146.07
z	0.121	0.125

Table 6. Lattice constants and position parameters for δ-$ZnCl_2$. For the space group $Pna2_1$, Zn and Cl atoms are located at general positions of (x, y, z), $\left(\bar{x}, \bar{y}, z+\frac{1}{2}\right)$, $\left(x+\frac{1}{2}, \bar{y}+\frac{1}{2}, z\right)$, $\left(\bar{x}+\frac{1}{2}, y+\frac{1}{2}, z+\frac{1}{2}\right)$ respectively. U (Å^2) gives the isotropic thermal amplitudes.

	This work				Experimental data [2]			
a (Å)	6.444				6.443			
b (Å)	7.666				7.693			
c (Å)	6.122				6.125			
β (deg)	90.0				90.0			
V (Å^3)	302.40				303.59			
Atom	x	y	z	U	x	y	z	U
Zn	0.081	0.125	0.378	0.0303	0.0818	0.1251	0.3750	0.0253
Cl	0.075	0.122	0.005	0.0296	0.0702	0.1223	0.0041	0.0305
Cl	0.084	0.630	0.003	0.0296	0.0841	0.6332	0.0062	0.0292

elastic energy resolution was about 15% of the initial energy. Several scans were performed with the final energy (E_f) values of 30 meV and $\mathbf{Q}$ values of 5–6 Å^{-1}, that are much larger than the size of the Brillouin zone (about 1 Å^{-1}). Additional measurements of the neutron background were made by detuning the analyser crystal from the position by $\pm 5^\circ$ and repeating the scan for the same sample.

The neutron weighted phonon density of states, $g^n(E)$, is obtained from the measured scattering function $S(\mathbf{Q}, E)$ through the following relation [26]:

$$g^n(E) = A\left\langle \frac{e^{2W(Q)}}{Q^2} \frac{E}{n(E,T)+1} S(\mathbf{Q}, E) \right\rangle \tag{1}$$

$$\approx B \sum_p \frac{4\pi b_p^2}{M_p} g_p(E) \tag{2}$$

where $n(E,T) = [\exp(E/KT) - 1]^{-1}$; A, B are normalization constants; $2W(Q)$ is the Debye–Waller factor; b_p, M_p and $g_p(E)$ refer respectively to the neutron scattering length, mass and partial phonon density of states of the pth atom in the unit cell. The quantity within $\langle \cdots \rangle$ represents the average over all $\mathbf{Q}$ values. The factor $\frac{4\pi b_p^2}{M_p}$ turns out to be 0.063 and 0.474 barn/amu for Zn and Cl atoms respectively.

4. Model interatomic potential

As previously stated, there is a need to formulate a realistic potential model that can effectively model the structure and dynamics in various polymorphs of $ZnCl_2$. In the present model, Born–Mayer repulsive and attractive van der Waals interactions among different pairs of atoms have

Table 7. Comparison of calculation and experimental data of optical modes in α-$ZnCl_2$. Modes of A_2 representation are not optically active.

	Optical phonon modes (cm^{-1})			
		Experimental data		
Representations	This work	[3]	[23]	[31]
A_1	223	226	233	245
A_2	147			
	301			
B_1	94	117		113
	273			
B_2	111	128		128
	325			
E	75	76	82	80
	99	100	103	103
	263			
	327			

Table 8. Comparison of calculation and experimental data of optical modes in β-$ZnCl_2$.

Optical phonon modes (cm^{-1})					
				Experimental data	
This work				[31]	[23]
A_g	B_g	A_u	B_u	(A_g, B_g)	(A_u, B_u)
34	33	34	36		
40	47	43	52		42
44	49	48	57		57
47	55	53	61		61
48	61	58	69		70
57	66	64	74		
64	71	70	84		
70	75	93	86	78	
72	79	94	100		99
90	91	108	107	104	105
102	104	110	116	108	
114	111	120	127	118	123
122	114	120	144	125	135
135	136	141	222		
148	138	216	232	231	
222	221	231	254	250	
241	236	252	257		
248	248	261	266	268	
261	260	264	273	278	
266	267	270	308		
273	268	308	317		
311	312	316	324		
315	320	324	326		
324	322	327	328		
327	327	328	340		
328	328	340			
340	340				

Table 9. Comparison of calculation and experimental data of optical modes in γ-$ZnCl_2$.

	Optical phonon modes (cm^{-1})		
		Experimental data	
Representations	This work	[3]	[31]
A_{1g}	244	248	252
A_{2u}	258		
B_{1g}	66		
	271		
B_{2u}	216		
E_g	44	36	38
	92	88	80
	322		
E_u	68		
	318		

Table 10. Comparison of calculation and experimental data of optical modes in δ-$ZnCl_2$.

Optical phonon modes (cm^{-1})					
This work				Experimental data	
A_1	A_2	B_1	B_2	[3]	[16]
45	50	50	72		39, 49, 59
75	55	67	91		74, 83, 88
92	76	108	118		96, 100, 102, 106
112	104	128	141	147	109, 124, 129
222	128	242	267		226, 250
264	235	270	269	278	272, 282
324	269	317	298		321
329	318	326	329		
	327				

been incorporated. Because of the covalent nature of the Zn–Cl bond, a stretching term has to be included further in the potential model. The model thus turns out to be

$$V(r) = A\exp\left[-\frac{Br}{R(k)+R(k')}\right] - \frac{C_{kk'}}{r^6} - D\exp\left[-\frac{n(r-r_0)^2}{2r}\right] \tag{3}$$

where A (=1822 eV) and B (=12.364) are two constants, used extensively in several previous works [27–29]; $R(k)$ and $R(k')$ refer to effective radius parameters for Zn and Cl atoms. $C_{kk'}$ accounts for van der Waals terms between Zn–Zn, Zn–Cl and Cl–Cl atoms; r_0 is the equilibrium Zn–Cl bond length; D and n are two adjustable parameters. At the observed lattice constants and atomic positions in the unit cell, the parameters were so adjusted as to give nearly a zero internal stress and net force on each individual atom. Once the structural constraints are met, the potential parameters were further adjusted so that the calculated eigenfrequencies are real for all the wavevectors in the entire Brillouin zone. The group theoretical analysis provides the symmetry vectors necessary for block diagonalization of the dynamical matrix. Table 2 lists the final values of the optimized parameters. All the necessary calculations were made using DISPR [30] developed at Trombay. Lattice parameters and atomic coordinates obtained as a result of the potential minimization for various polymorphs of $ZnCl_2$ are displayed in tables 3–6. At high pressures, the equilibrium crystal structures were obtained from the free energy minimization.

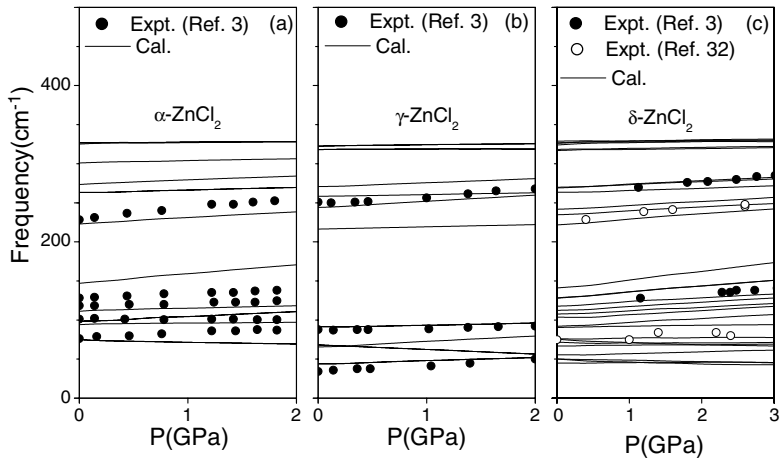

Figure 2. Pressure dependence of phonon modes in (a) α-$ZnCl_2$, (b) γ-$ZnCl_2$ and (c) δ-$ZnCl_2$.

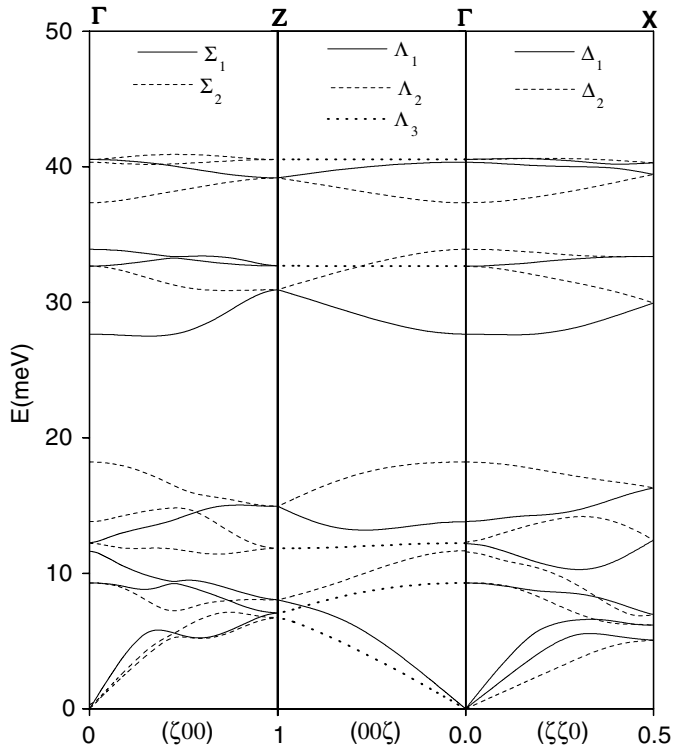

Figure 3. Calculated phonon dispersion relations in α-$ZnCl_2$.

5. Vibrational modes: Raman and infrared active

A group theoretical classification of various zone-centre phonon modes for each of the crystalline modifications in $ZnCl_2$ is given in table 1. Experimental mode assignments are available for only two polymorphs of $ZnCl_2$ (namely α-$ZnCl_2$ and γ-$ZnCl_2$). Measured optical

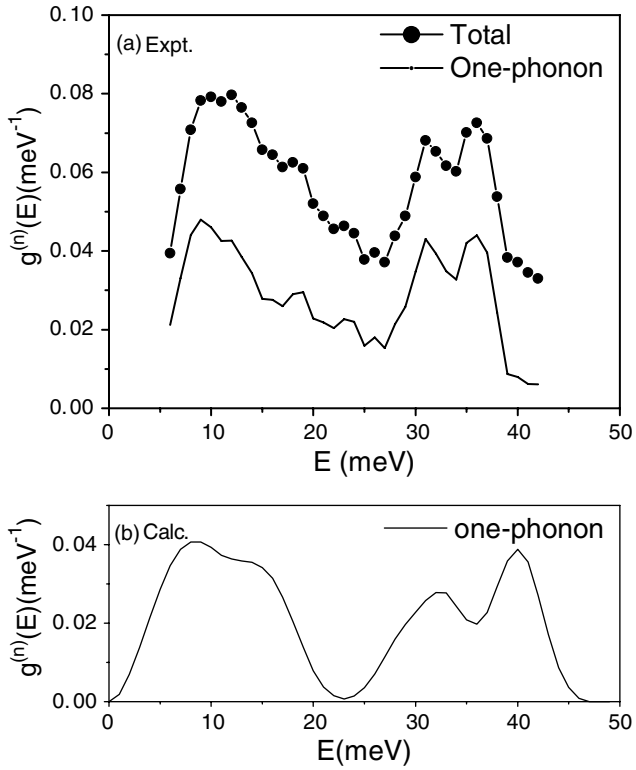

Figure 4. Plots of (a) experimental and (b) calculated neutron weighted phonon density of states for α-$ZnCl_2$. The multiphonon contribution at 300 K has been subtracted from the experimental data to obtain the experimental one-phonon spectrum. The corresponding calculated spectrum has been convoluted with the energy resolution of the instrument.

phonon data [3, 16, 23, 31] are found to be in good agreement with our calculated results (tables 7–10). It may be noted that the lowest frequency mode in the γ-phase (36 cm^{-1}) is almost half the frequency of that in the α-phase (80 cm^{-1}). Further, the pressure dependence of Raman modes in α, γ and δ forms of $ZnCl_2$ are calculated. Except for the α-phase, in all the others, the calculated pressure dependence compares well with the available measured [3, 32] data (see figure 2). Since β-$ZnCl_2$ has as many as 108 phonon modes, the pressure dependence of these modes is not shown here.

6. Phonon dispersion relations and phonon density of states in α-$ZnCl_2$

As table 1 suggests, there is a total of 18 degrees of freedom in α-$ZnCl_2$, giving rise to 18 phonon frequencies. Following are the representations of normal modes along the three high symmetry directions (namely Σ, Λ and Δ).

$$\Sigma(100): 8\Sigma_1 + 10\Sigma_2$$
$$\Lambda(001): 4\Lambda_1 + 4\Lambda_2 + 5\Lambda_3 \qquad (\Lambda_3 \text{ being doubly degenerate})$$
$$\Delta(110): 9\Delta_1 + 9\Delta_2.$$

Figure 3 displays the calculated phonon dispersion relations in α-$ZnCl_2$. Considerable dispersion and anti-crossing are found for the branch in all the three symmetry directions

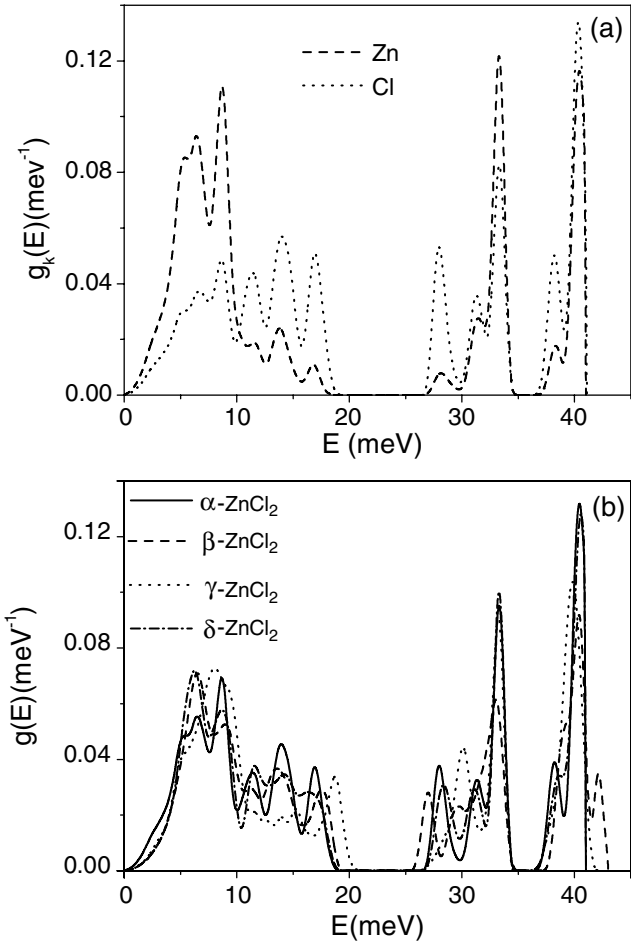

Figure 5. (a) Calculated partial phonon density of states of various atoms in α-$ZnCl_2$. (b) A comparison of calculated one-phonon density of states in various crystalline polymorphs of $ZnCl_2$.

which indicate strong hybridization. There are no indications of any phonon softening in the calculations in any of the four polymorphs at ambient pressure.

We have plotted the measured phonon density of states along with the calculated spectrum in figure 4. The experimental one-phonon spectra are obtained by subtracting the multiphonon contribution from the experimental data. The multiphonon contribution is obtained using the Sjolander formalism [33]. The experimental data (figure 4) confirm two broad structures with a bandgap around 25 meV. However, frequencies around 20 meV seem to be underestimated in the calculations. The measured neutron data [34] for vitreous $ZnCl_2$ and the Raman density of states data [35] for molten $ZnCl_2$ are qualitatively similar to the present neutron data on crystalline α-$ZnCl_2$.

The computed partial phonon density of states is shown in figure 5(a). This indicates that the Zn ions contribute significantly at energies below 10 meV while from 10 to 19 meV the vibrations of Cl ions dominate. However, in the higher energy region, contributions from both the ions remain more or less similar. A comparison of the calculated phonon density of states for all the crystalline polymorphs is shown in figure 5(b). Two bandgaps (a broad one around

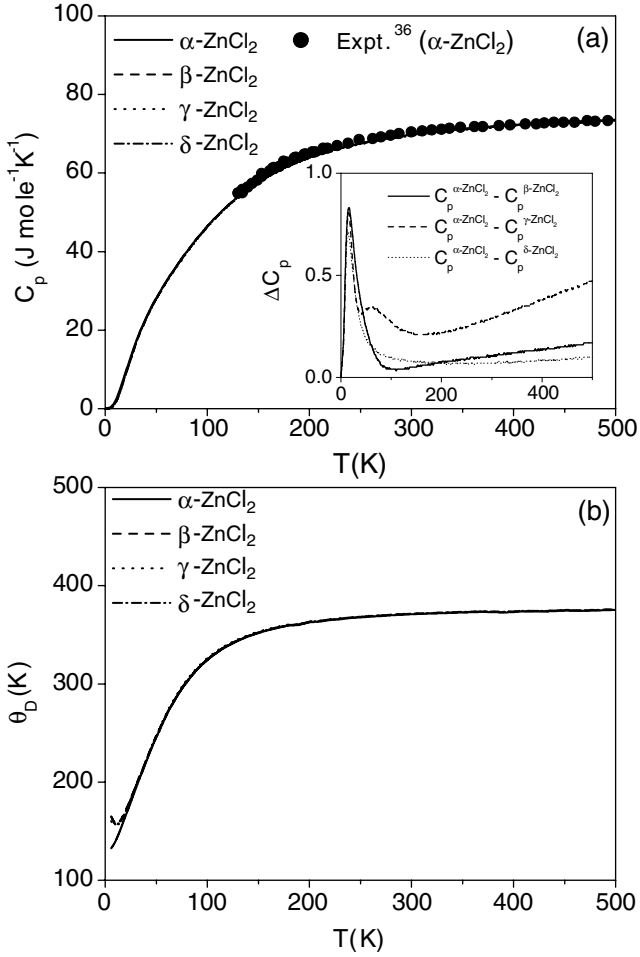

Figure 6. Plots of (a) heat capacity (C_p) and (b) Debye temperature (θ_D) for all the crystalline polymorphs of $ZnCl_2$. The inset in (a) shows the specific heat differences of various polymorphs with respect to the α-phase.

23 meV and a very narrow one around 36 meV) are observed in each of the phases, though of slightly varying degree. For these calculations, all the phonon modes are integrated at each wavevector within the irreducible Brillouin zone on a $10 \times 10 \times 10$ mesh with an energy resolution of 1.0 meV.

7. Thermodynamic properties

7.1. Heat capacity and Debye temperature

As figure 6(a) suggests, there is a fairly good agreement between the calculated and the experimental data [36] on the molar heat capacity. As the inset shows, there is very small variation among heat capacities of various polymorphs, which reflects the small variation in the respective phonon density of states. In particular, the spike in ΔC_p at about 50 K in the inset of figure 6(a) arises due to the different phonon density of states of the α-phase at low energy in figure 5(b). Figure 6(b) displays the Debye temperature (θ_D) plot for different crystalline

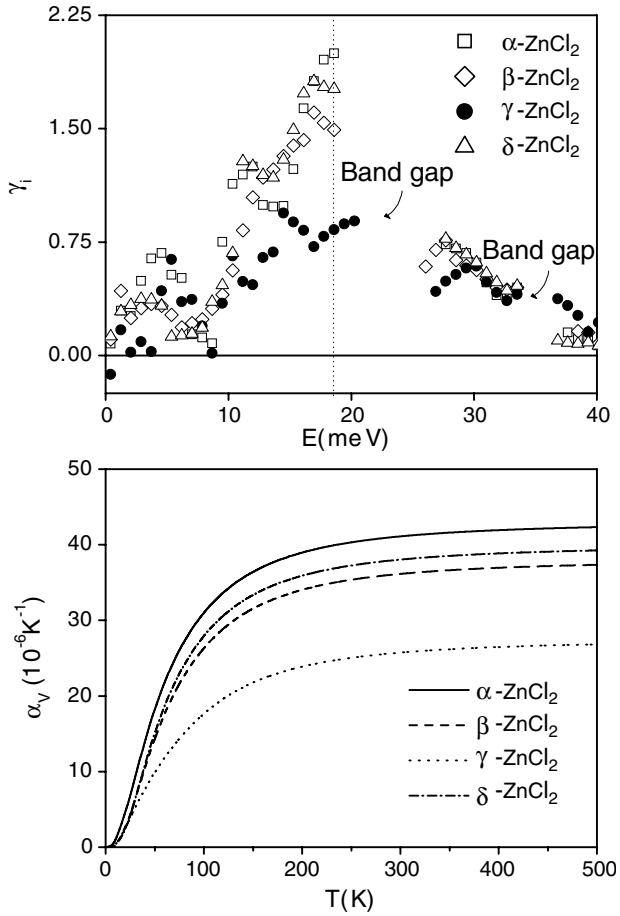

Figure 7. Calculated plots of the mode Grüneisen parameter and the volume thermal expansion coefficients of $ZnCl_2$ in its various crystalline phases.

modifications in $ZnCl_2$. The characteristic Debye temperature in the present model turns out to be 375 K, while the experimental value is 340 K [36].

7.2. Mode Grüneisen parameters and thermal expansion

The mode Grüneisen parameters are important indicators of the anharmonicity of phonon modes and their role in determining the thermal expansion. For the ith mode the Grüneisen parameter is given by

$$\gamma_i = -\frac{\partial \ln \omega_i}{\partial \ln V}. \tag{4}$$

In the quasiharmonic approximation, the ith phonon mode contributes $(\frac{1}{BV})\gamma_i C_{Vi}$ to the volume thermal expansion (α_V), where C_{Vi} denotes the contribution of the ith mode to the volume heat capacity. As heat capacity and bulk modulus values remain similar for each of the polymorphs, it is obviously the mode Grüneisen parameter which dominates in the determination of α_V. Figure 7 displays averaged γ_i as a function of phonon energy for different crystalline polymorphs in $ZnCl_2$. One may notice that, while for α, β and δ phases 18 meV

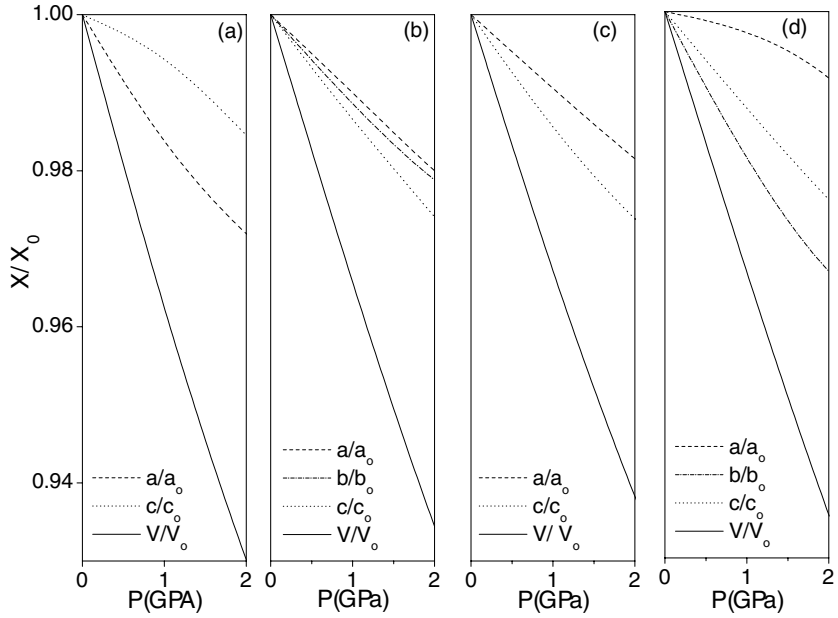

Figure 8. Calculated equations of state for crystalline $ZnCl_2$ in (a) α, (b) β, (c) γ and (d) δ phases.

phonons have maximum variations with volume, γ-$ZnCl_2$ behaves slightly differently. This is further reflected in the subsequent thermal expansion calculation (see figure 7).

7.3. Equation of state

The crystal structure parameters as a function of pressure (at $T = 0$ K) are calculated corresponding to the minimum of Gibbs free energy. Figure 8 shows how the cell dimensions belonging to different crystalline polymorphs of $ZnCl_2$ vary with pressure. It is observed that the compressibility is anisotropic. While the **c** axis is the most compressible in β and γ forms of $ZnCl_2$, it is the least compressible in α-$ZnCl_2$. In δ-$ZnCl_2$, the **b** axis is found to be the most compressible. However, the volume derivative with pressure in all the phases looks a bit alike, as their bulk moduli are similar.

8. Conclusions

We have developed an interatomic potential model for $ZnCl_2$ that mimics the vibrational and thermodynamic properties of the polymorphs of crystalline $ZnCl_2$ and reproduces fairly well the inelastic neutron scattering data for the α-phase. The fact that the γ-phase shows differences in Grüneisen parameters and lattice expansion is essentially due to its layered structure, which is very different from other corner-shared polymorphs. This transferable potential model may further be exploited to investigate the properties of the glassy and the liquid phases of $ZnCl_2$.

Acknowledgments

AS expresses his gratitude to the Council of Scientific and Industrial Research (CSIR, New Delhi), India, for rendering the financial assistance and acknowledges as well the

encouragement and care taken by Dr M Ramanadham and Dr V C Sahni. We thank Dr S N Achary for his kind cooperation in making the commercial polycrystalline $ZnCl_2$ sample suitable for the inelastic neutron scattering experiments. We are also grateful to the referees for their valuable comments.

References

[1] Brehler B 1961 *Z. Kristallogr.* **115** 373
[2] Brynestad J and Yakel H L 1978 *Inorg. Chem.* **17** 1376
[3] Sakai M, Kuroda N and Nishina Y 1985 *J. Phys. Soc. Japan* **54** 4081
[4] Gardner P J and Heyes D M 1985 *Physica* B **131** 227
[5] McKenzie J D and Murphy W K 1960 *J. Chem. Phys.* **33** 366
[6] Gruber G J and Litovitz T A 1964 *J. Chem. Phys.* **40** 13
[7] Woodcock L V, Angell C A and Cheeseman P 1976 *J. Chem. Phys.* **65** 1565
[8] Bockris J O' M, Richards S R and Nanis I 1965 *J. Phys. Chem.* **69** 1627
[9] Duke F R and Fleming R A 1957 *J. Electrochem. Soc.* **104** 251
[10] Ribero M C C, Wilson M and Madden P A 1999 *J. Chem. Phys.* **110** 4803
[11] Smith G P and Triolo R 1981 *J. Chem. Phys.* **75** 613
[12] O'Bryan H M Jr, Van Uitert L G, Guggenheim H J and Grodkiewicz W H 1979 *Bull. Am. Ceram. Soc.* **58** 1098
[13] Lebon M J, Drefus C, Li G, Housadi A, Cummins H Z and Pick R M 1995 *Phys. Rev.* E **51** 4357
[14] Kartini E, Collins M F, Mezei F and Svensson E C 1997 *Physica* **234** 399
[15] Ribero M C C, Wilson M and Madden P A 1998 *J. Chem. Phys.* **109** 9859
[16] Yannopoulos S N, Kalampounias A G, Chrissanthopoulos A and Papatheodorou G N 2003 *J. Chem. Phys.* **118** 3197
[17] Angell C A, Wegdam G and van der Elsken J 1974 *Spectrochim. Acta* A **30** 665
[18] Triolo R and Narten A H 1981 *J. Chem. Phys.* **74** 703
[19] Desa J A E, Wright A C, Wong J and Sinclair R N 1982 *J. Non-Cryst. Solids* **51** 57
[20] Pauling L 1929 *Proc. Natl Acad. Sci. USA* **15** 709
[21] Oswald H R and Jaggi H 1960 *Helv. Chim. Acta* **43** 72
[22] Yakel H L and Brynestad J 1978 *Inorg. Chem.* **17** 3294
[23] Angell C A and Wong J 1970 *J. Chem. Phys.* **53** 2053
[24] Young R A, Sakthivel A, Moss T S and Paiva-Santos C O 1995 *J. Appl. Crystallogr.* **28** 366
[25] Chaplot S L, Mukhopadhyay R, Vijayaraghavan P R, Deshpande A S and Rao K R 1989 *Pramana J. Phys.* **33** 595
[26] Price D L and Skold K 1986 *Neutron Scattering* vol A, ed K Skold and D L Price (Orlando, FL: Academic)
Carpenter J M and Price D L 1985 *Phys. Rev. Lett.* **54** 441
Taraskin S N and Elliott S R 1997 *Phys. Rev.* B **55** 117
[27] Chaplot S L 1992 *Phys. Rev.* B **45** 4885
[28] Rao Mala N, Chaplot S L, Choudhury N, Rao K R, Azuah R T, Montfrooij W T and Bennington S M 1999 *Phys. Rev.* B **60** 12061
[29] Mittal R, Chaplot S L, Sen A, Achary S N and Tyagi A K 2003 *Phys. Rev.* B **67** 134303
[30] Chaplot S L, unpublished
[31] James D W, Parry R M and Leong W H 1978 *J. Raman Spectrosc.* **7** 71
[32] Polski C H, Martinez L M, Leinenweber K, VerHelst M A, Angell C A and Wolf G H 2000 *Phys. Rev.* B **61** 5934
[33] Sjolander A 1958 *Ark. Fys.* **14** 315
[34] Galeener F L, Mikkelsen J C Jr, Wright A C, Sinclair R N, Desa J A E and Wong J 1980 *J. Non-Cryst. Solids* **42** 23
[35] Aliotta F, Maisano G, Migliardo P, Vasi C, Wanderlingh F, Smith G P and Triolo R 1981 *J. Chem. Phys.* **75** 613
[36] Angell C A, Williams E, Rao K J and Tucker J C 1977 *J. Chem. Phys.* **81** 238